Carbohydrate Polymers 95 (2013) 64–71

Contents lists available at SciVerse ScienceDirect

Carbohydrate Polymers

journal homepage: www.elsevier.com/locate/carbpol

Blood compatibility of polyethersulfone membrane by blending a sulfated derivative of chitosan

Jimin Xue, Weifeng Zhao, Shengqiang Nie, Shudong Sun*, Changsheng Zhao

College of Polymer Science and Engineering, State Key Laboratory of Polymer Materials Engineering, Sichuan University, Chengdu 610065, People's Republic of China

ARTICLE INFO

Article history:
Received 1 August 2012
Received in revised form 4 February 2013
Accepted 15 February 2013
Available online 26 February 2013

Keywords:
Chitosan
Polyethersulfone
Blood compatibility

ABSTRACT

In this study, a novel sulfated derivative of chitosan, which could be dissolved in many common organic solvents, is conveniently synthesized for the modification of polyethersulfone (PES) membrane. Elemental analysis, FTIR, ^{1}H NMR and X-ray diffraction diagrams (XRD) are used to demonstrate the introduction of functional groups. Owing to the solubility in organic solvents, the sulfated derivative of chitosan could be directly blended with PES in organic solvent to prepare membrane by means of a liquid–liquid phase separation technique. The modified membrane showed lower protein (bovine serum albumin (BSA) and bovine serum fibrinogen (BFG)) adsorption and suppressed platelet adhesion. Moreover, the activated partial thromboplastin time (APTT) for the modified membrane was enhanced as high as 60% compared to pure PES membrane. The lower protein adsorption, suppressed platelet adhesion and increased APTT confirmed that the blood compatibility of the modified PES membrane by the sulfated derivative of chitosan was significantly improved.

1. Introduction

In order to achieve a further controlled modification reaction of chitosan or to obtain some modification reactions in homogeneous conditions smoothly, phthaloylation reaction was carried out (Kurita, Ikeda, Yoshida, Shimojoh, & Harata, 2002; Nishimura, Kohgo, Kurita, & Kuzuhara, 1991), since the product of phthaloylated chitosan was a particularly convenient organosoluble precursor for efficient modifications.

The sulfated chitosan is one kind of the most important products of different modifications of chitosan due to the numerous applications, such as post-treatment of wastewater, anticoagulant, adipogenesis inhibition and antibacterial (Chaudhari & Murthy, 2011; Huang, Du, Zheng, Liu, & Fan, 2004; Karadeniz, Karagozlu, Pyun, & Kim, 2011; Muzzarelli et al., 1984). It is noteworthy that the structure of sulfated derivatives of chitosan is similar to that of heparin, a natural blood anticoagulant. Several studies about the anticoagulant activity of sulfated chitosan had been reported (Muzzarelli & Giacomelli, 1987; Vikhoreva et al., 2005; Vongchan, Sajomsang, Subyen, & Kongtawelert, 2002; Yang et al., 2012), however, few of these sulfated derivatives of chitosan were organosoluble, which are likely to restrict the applications in some specific areas.

In order to expand the applications of the sulfated derivatives of chitosan and obtain an improved blood compatible material, a novel organosoluble sulfated derivative of chitosan was synthesized for the modification of PES membrane in this study. As one of the most important polymeric materials, PES is widely used in separation fields and biomedical fields such as artificial organs and medical devices used for blood purification (Samtleben, Dengler, Reinhardt, Nothdurft, & Lemke, 2003; Zhao & Li, 2001); however, the blood compatibility of PES membrane was not adequate. Ran et al. (2011) modified PES membrane by blending an amphiphilic triblock co-polymer, Sperling, Houska, Brynda, Streller, and Werner (2006) coated albumin–heparin multilayer coatings on PES membrane by layer-by-layer technique, and Fang et al. (2009) grafted bovine serum albumin onto the surface of PES/poly (acrylonitrile-co-acrylic acid) blended membrane to improve the blood compatibility. It is well accepted that blending is the simplest way to modify PES membranes compared with other methods, and thus widely used in industrial fields.

In the present study, a novel sulfated derivative of chitosan was synthesized through a simple method. Then, the sulfated derivative of chitosan was used as a macromolecular additive for direct blending with PES to prepare modified PES membranes by a phase inversion technique, and the surface properties (surface compositions and water contact angles), blood compatibility (protein adsorption, platelet adhesion and clotting time)

* Corresponding author. Tel.: +86 28 85400453; fax: +86 28 85405402.
E-mail addresses: stephen9988@126.com (S. Sun), zhaochsh70@163.com, zhaochsh70@scu.edu.cn (C. Zhao).

0144-8617/$ – see front matter © 2013 Elsevier Ltd. All rights reserved.
http://dx.doi.org/10.1016/j.carbpol.2013.02.033

and the ultrafiltration property of the modified membranes were investigated.

2. Experimental

2.1. Materials

PES (Ultrason E6020P) was obtained from BASF, Germany. *N*,*N*-Dimethylacetamide (DMAc) (AR, 99.0 wt.%) and *N*,*N*-dimethylformamide (DMF) (99.0 wt.%) were purchased from Chengdu Kelong Inc. (China), which were purified with vacuum distillation over CaH_2, and used as the solvents. Bovine serum albumin (BSA) and bovine fibrinogen (BFG) were obtained from Sigma Chemical Company. Chitosan (C) (M_w: 60 kDa; DD: 90%; the deacetylation degree (DD) of chitosan samples was determined by alkalimetry) was obtained from Shanghai Bio Science & Technology Corp. (China). *O*-Phthalic anhydride was purchased from Chengdu Kelong Inc. (China). Spectra/Por Dialysis membrane (MWCO 8000–14,000) was purchased from Chengdu Kebite Biotechnologies Co. Ltd. (China). All the other chemicals (analytical grade) were obtained from Chengdu Kelong Inc. (China), and were used without further purification.

2.2. Synthesis and characterization of the derivative of chitosan

2.2.1. Synthesis of phthaloylated chitosan and sulfonated phthaloylated chitosan derivatives

O-Phthalic anhydride (3.6 g) and chitosan (2 g) were dissolved in 40 mL of mixed solvent (DMF/water, 97/3, v/v), and the reaction was performed at 120 °C under nitrogen atmosphere with stirring for 5 h. Then, the resulting mixture was cooled to room-temperature and diluted with DMF (20 °C); After that, the solution was centrifugated at 8000 rpm for 10 min to remove the insolubles, the supernatant solution was collected and dialyzed against ethanol for 72 h, and then against double distilled water for 72 h; the resulting suspension was freeze-dried. Then organic soluble chitosan (OC) was obtained. In order to investigate the effect of the phthaloylation on the degree of sulfation, the reaction was also conducted in DMF without water, and the product was marked as OC1.

Chlorosulfonic acid, the most commonly used sulfating reagent, was adopted to synthesize the sulfated derivative of chitosan. Chlorosulfonic acid (20 mL) was added dropwise into DMF (20 mL) with stirring at 0 °C under N_2 atmosphere and kept agitating for 1 h; then a solution of OC (0.5 g) and DMF (20 mL) was added. The mixture was reacted under N_2 atmosphere for 24 h at 20 °C. The crude solution was neutralized with 20 wt.% NaOH solution to pH = 7, and dialyzed against double distilled water; then the resulting suspension was freeze-dried, and the final powder was named as SOC. Moreover, SOC1 was synthesized from the OC1 in the same way.

The reaction pathway is shown in Fig. 1.

2.2.2. Characterization

The FTIR spectra were recorded with KBr pellets on a Nicolet-560 spectrophotometer (USA). 32 scans at a resolution of 4 cm^{-1} were averaged and referenced against air.

^1H NMR (400 MHz) spectra were recorded on a Bruker AVII-400MHz spectrometer (Bruker Co., Germany), using tetramethylsilane (TMS) as the internal standard in DMSO-d_6 at room temperature.

Elemental analysis, which is based on the determination of carbon (C), hydrogen (H), nitrogen (N) and sulfur (S), was performed using a CARLO ERBA 1106 elemental analyzer (Italy), with a carrier gas (He, at a flow rate of 100 mL min^{-1}) at a combustion temperature of 1000 °C using the solid samples.

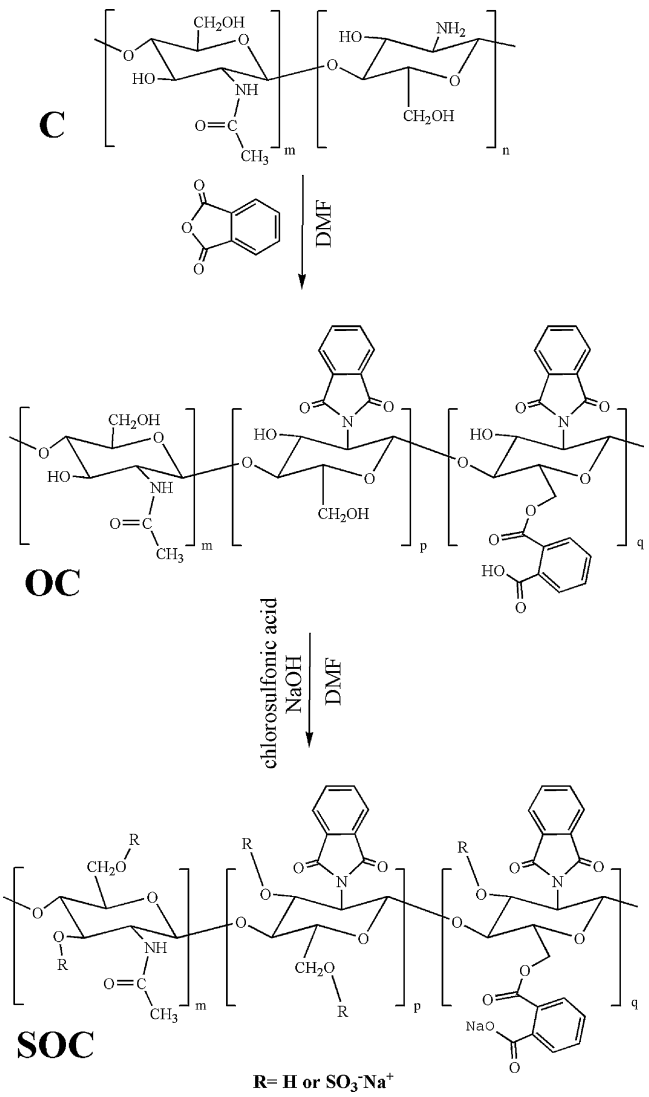

Fig. 1. Mechanism of the synthesis of the sulfated derivative of chitosan (SOC).

X-ray diffraction diagrams were obtained by the powder method with the use of Ni-filered Cu Kα radiation with an X'Pert Pro MPD instrument (Philips, Holland).

2.3. Preparation and characterization of modified membranes

The modified membranes were prepared by a phase inversion technique. PES and the synthesized derivatives of chitosan were dissolved in DMAc by vigorous stirring. In the study, the concentration of PES was kept at 16 wt.%, and the weight percentage of SOC or OC in the casting solutions was varied. The content of SOC/OC in the casting solutions was 0, 1, 2, and 4 wt.% respectively. After vacuum degassing, the casting solutions were prepared into membranes by spin coating coupled with a liquid–liquid phase separation technique at room temperature as the method mentioned in the literature (Matsuyama, Nishiguchi, & Kitamura, 2000). The membranes were thoroughly rinsed with distilled water to remove the residual solvent. The prepared membranes with PES/SOC ratios of 16/0, 16/1, 16/2, and 16/4 (wt.%) were termed M0, M1, M2, and M4; the membranes with PES/OC (as control samples) ratios of 16/1, 16/2, and 16/4 (wt.%) were termed P1, P2, and P4, respectively (compositions are shown in supplementary Table S1).

Attenuated total reflection-Fourier transform infrared spectra (ATR-FTIR) for the surfaces of membranes were obtained by a

Fourier-transform infrared spectrometer (Nicolet 560, America) with an incidence angle of 90°.

X-ray photoelectron spectroscopy (XPS) surface element analysis of the membranes was performed using a KRATOS XSAM800 Britain XPS Instrument, employing Al Kα excitation radiation (1486.6 eV). The measurements were conducted at the take-off angle of 20°.

Contact angles were measured with a contact angle goniometer (OCA20, Dataphysics, Germany). The stationary, advancing and receding contact angles of membranes were measured on 3 μL of double distilled water at 20 °C, and the results reported are the mean values of five replicates.

The morphology of the membranes was observed by scanning electron using a JSM-7500F scanning microscope (JEOL, Japan).

2.4. Blood compatibility

2.4.1. Protein adsorption

Protein adsorption experiments were carried out with BSA and BFG solutions under the static condition. Firstly, the membrane with an area of 1 cm × 1 cm was immersed in a phosphate buffer solution (PBS), containing BSA or BFG with the concentration of 1 mg/mL, and incubated at 37 °C for 1 h; then the membrane was rinsed slightly with PBS solution and double distilled water. Then the membrane was placed in a washing solution (2% sodium dodecyl sulfate (SDS) and 0.05 M NaOH) at 37 °C, and shaken for 2 h to remove the adsorbed protein. The adsorption and desorption times were carefully determined in preliminary experiments. The protein concentration in the washing solution was determined by using the Micro BCA™ Protein Assay Reagent Kit (PIERCE), and then the adsorbed protein amount was calculated.

2.4.2. Platelet adhesion

In order to eliminate the interference of other components in blood, such as erythrocyte and leucocyte, platelet-rich-plasma (PRP) was used for studying platelet adhesion on the PES membranes. Healthy human fresh blood (man, 30 years old) was collected using vacuum tubes, containing sodium citrate as an anticoagulant (anticoagulant to blood ratio, 1:9, v/v), and PRP was obtained after centrifuging at 1000 rpm for 15 min. The membranes were immersed in PBS (pH = 7.2–7.4) and equilibrated at 37 °C for 1 h. The PBS was removed, and then 1 mL of fresh PRP was introduced. The membranes were incubated with PRP at 37 °C for 30 min. Then the PRP was decanted off and the membranes were rinsed 3 times with PBS. Finally, the membranes were treated with 2.5 wt.% glutaraldehyde in PBS at 4 °C for 24 h. The samples were washed with PBS, subjected to a drying process by passing them through a series of graded alcohol–PBS solutions (30, 50, 70, 80, 90, 95 and 100%, v/v). The critical point drying of the specimens was done with liquid CO_2. The platelet adhesion was observed using a JSM-7500F microscope (JEOL).

2.4.3. Clotting time

To evaluate the antithrombogenicity of the derivatives of chitosan and the blended membranes, activated partial thromboplastin time (APTT) and thrombin time (TT) were measured by an automated blood coagulation analyzer CA-50 (Sysmex Corporation, Kobe, Japan), and the test method was described as follows: healthy human fresh blood (man, 30 years old) was collected using vacuum tubes, containing sodium citrate as an anticoagulant (anticoagulant to blood ratio, 1:9, v/v). The platelet-poor plasma (PPP) was obtained after centrifuging at 4000 rpm for 15 min. Synchronously, the derivatives of chitosan and the membranes (0.5 cm × 0.5 cm, three pieces) were immersed in PBS (0.2 mL, pH = 7.4) for 1 h. Then the PBS was removed and 0.1 mL of fresh PPP was introduced. After incubating at 37 °C for 30 min, 50 μL of the incubated PPP was added into the test cup, followed by the addition of 50 μL of APTT agent (incubated 10 min before use) and incubation at 37 °C for 3 min. Thereafter, 50 μL of 0.025 M $CaCl_2$ solution was added, and then the APTT was measured. For the TT test, 50 μL of TT agent was added into the test cup (containing 50 μL of the incubated PPP) after 10 min incubating, and then the TT was measured. At least three measurements were averaged to get a reliable value, and the results were analyzed by statistical method.

2.5. Permeation and antifouling property

The water flux, protein antifouling property, and water flux recovery ratio of the membranes were assessed by ultrafiltration experiments. A dead-end ultrafiltration cell was used, in which the effective membrane area was 13.8 cm^2.

Firstly, the membranes were pre-compacted by double distilled water for 30 min to get steady filtration. Then, the water flux (F) was determined at room temperature and calculated using the equation: $F = V/SPT$, where V is the volume of the permeated solution (mL); S is the effective membrane area (m^2); P is the pressure applied to the membrane (mmHg) and T is the time (h).

After the filtration of water, the feed was switched to 1 mg/mL BSA/water solution to determine protein rejection ratio (R), which was defined as follows: $R\ (\%) = (1 - C_p/C_b) \times 100$, where C_p and C_b (mg/mL) are the BSA concentrations in the permeated and bulk solutions, respectively. The BSA concentrations were measured by a UV–vis spectrophotometer at the wavelength of 278 nm. The flux of BSA solution was also measured.

After BSA filtration, the membranes were rinsed with flowing double distilled water for 30 min. Then, the water flux was measured again and the recovery ratio (F_{RR}) of the membrane was calculated using the following expression: $F_{RR}\ (\%) = (F_2/F_1) \times 100$, where F_1 and F_2 (mL/(mmHg h m^2)) are the water flux before and after BSA filtration, respectively.

The tests were repeated three times for each sample to get a reliable value, and the results were expressed as means ± SD.

3. Results and discussion

3.1. Synthesis and characterization of the derivatives of chitosan (OC and SOC)

The mechanism for the synthesis of the derivatives of chitosan (OC and SOC) is shown in Fig. 1. The synthesizing process included two steps: the synthesis of the key intermediate (OC) and the synthesis of the sulfated derivative chitosan (SOC).

In this study, two kinds of phthaloylated chitosan were synthesized. OC was synthesized in a mixed solvent of DMF and water (97:3 in v/v), while OC1 was synthesized in DMF. As shown in Table 1, the degree of substitution (DS) for the OC dramatically reduced compared with the OC1, which was caused by the water in the mixed solvent. It was well known that the phthaloylation

Table 1
Element analysis results and the degree of substitution.

Sample	Elemental analysis (wt.%)				Degree of substitution
	C%	H%	N%	S%	
OC1	56.2	5.71	3.15	0	1.46[a]
OC	52.32	4.49	3.41	0	1.12[a]
SOC1	58.7	4.28	3.28	2.21	0.66[b]
SOC	53.8	3.42	3.54	3.44	0.96[b]

[a] Substitution degree of phthaloylation of chitosan was calculated according to the C/N (wt.%) from the element analysis.
[b] Substitution degree of the sulfation of chitosan was calculated according to the S/N (wt.%) from the element analysis.

of chitosan in DMF always accompanied by *O*-phthaloylation, and the solubility of the phthaloylated chitosan in organic solvents was owing to the coexistence of *N*-phthaloyl and *O*-phthaloyl groups (Kurita et al., 2002). However, on the other hand, the *O*-phthaloyl group is an obstacle to quantitative and regioselective substitution for further modification. Kurita et al. found that the DS of phthaloylation of chitosan decreased with the increase of reaction time, and the addition of cosolvent (water) could reduce the DS. The results indicated that the addition of water to the solvent could reduce the amount of *O*-phthaloyl groups of the product. Thus, in order to obtain a phthaloylated chitosan with low *O*-phthaloyl group content for further modification (sulfation) and high solubility in organic solvents, water was added to the solution.

For the sulfation step, both OC and OC1 were sulfated by chlorosulfonic acid in a homogeneous solution. It could be observed from Table 1 that the degree of sulfation of SOC was higher than that of SOC1, revealing an opposite trend to the DS of phthaloylation of chitosan, mostly due to the reduced amount of *O*-phthaloyl groups.

The structure changes of chitosan and the derivatives of chitosan were confirmed by FTIR. As shown in Fig. 2A, compared to the IR spectrum of chitosan, the spectra of OC and OC1 showed new peaks at 1778 and 1710 cm^{-1}, which were attributed to C=O bonds from the imide groups; and the new peak at 720 cm^{-1} was assigned to the out-of-plane deformation of the C—H bonds in the 1,2-disubstituted benzene rings. It indicated that the phthaloylated chitosan was synthesized. Moreover, some differences between OC and OC1 were found, for the OC1 obtained in DMF, the weak band at 2600–2700 cm^{-1} could attribute to the free carboxyl, and the medium peak at 1290 was assigned to ester bonds; while for the OC prepared in DMF/water, the peak at 1290 cm^{-1} was very weak due to the low amount of the *O*-phthaloyl groups, which was in agreement with the results of the element analysis.

Fig. 2B shows the FTIR spectra of chitosan and the derivatives of chitosan. Compared to OC, the spectrum of SOC showed a new peak at 1227 cm^{-1} which was assigned to the O=S=O groups. Therefore, it could be concluded that the sulfate groups were grafted onto OC.

The ^{1}H NMR (DMSO-d_6) spectra of OC and OC1 are shown in Fig. 2C. The peak near 2 ppm was assigned to methyl hydrogen (s, $HNCOCH_3$), and the peaks at 3.0–5.0 ppm were attributed to the hydrogen of pyranose ring (m, C_1–C_6). The obvious changes were observed in the proton peaks at 7–8 ppm and 13 ppm. Compared to the OC1, the areas of *O*-Phth and carboxy hydrogen (s, COOH) of OC decreased in the spectrum, which confirmed that the amount of *O*-phthaloyl groups of OC was smaller than that of OC1.

Fig. 2D shows the X-ray diffraction diagrams of chitosan and its derivatives. Chitosan has two reflections at $2\theta = 10.4^\circ$ and $2\theta = 20^\circ$, corresponding to the L-2 polymorph of chitosan. (Saito, Tabeta, & Ogawa, 1987). However, for OC and SOC, the reflections at $2\theta = 10.4^\circ$ and $2\theta = 20^\circ$ disappeared, which meant that the OC and SOC were amorphous structures. The heterogeneous structure was owing to the coexistence of un-deacetylated units, partial *O*-phthaloyl groups and the bulkiness of the *N*-phthaloyl groups. Furthermore, significant amorphous structure for the sulfated derivative of chitosan (SOC) was observed compared with that for the OC.

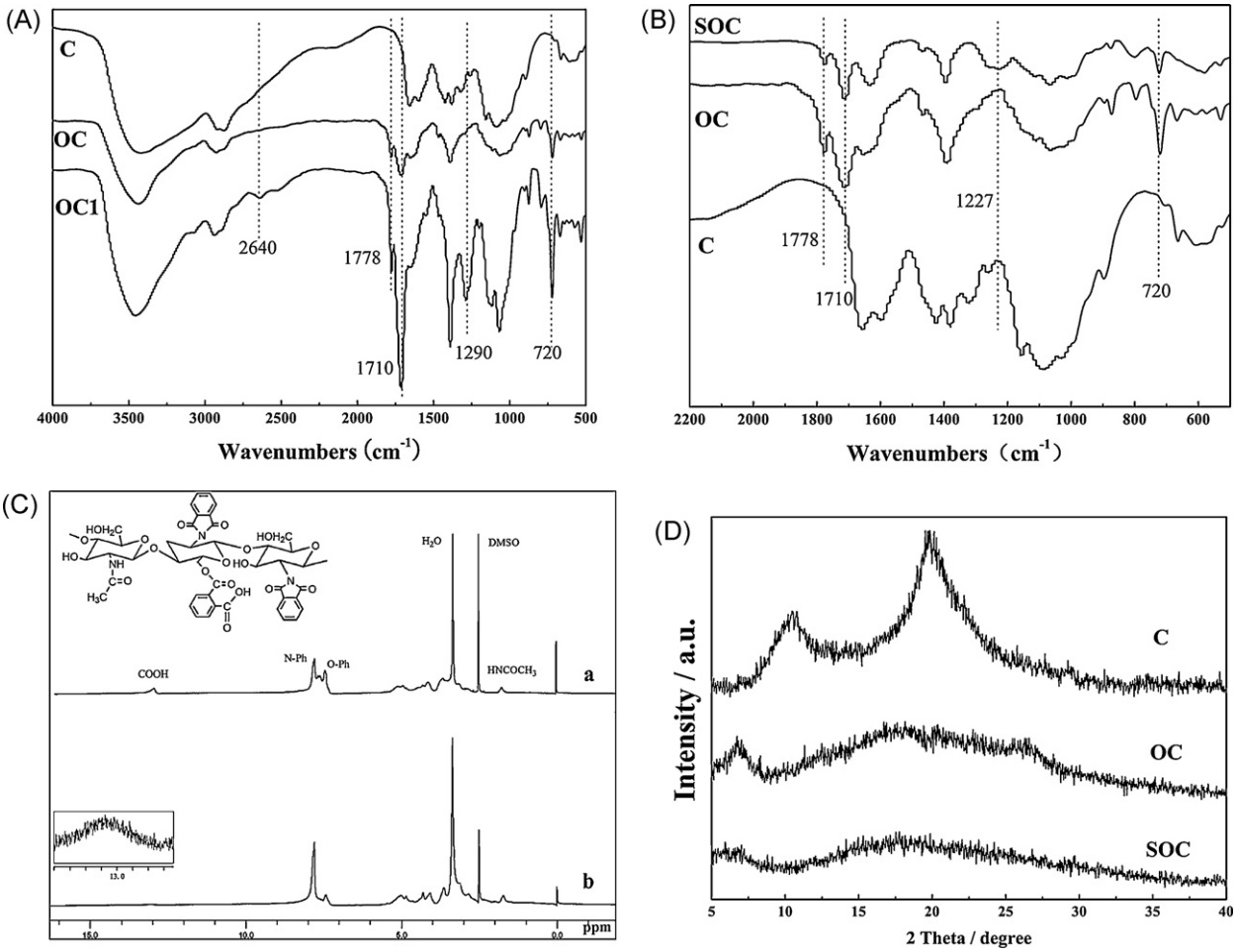

Fig. 2. (A) FTIR spectra of C, OC and OC1; (B) FTIR spectra of C, OC and SOC; (C) ^{1}H NMR spectra of the derivatives of chitosan: (a) OC1 and (b) OC; and (D) X-ray diffraction diagrams of chitosan and its derivatives.

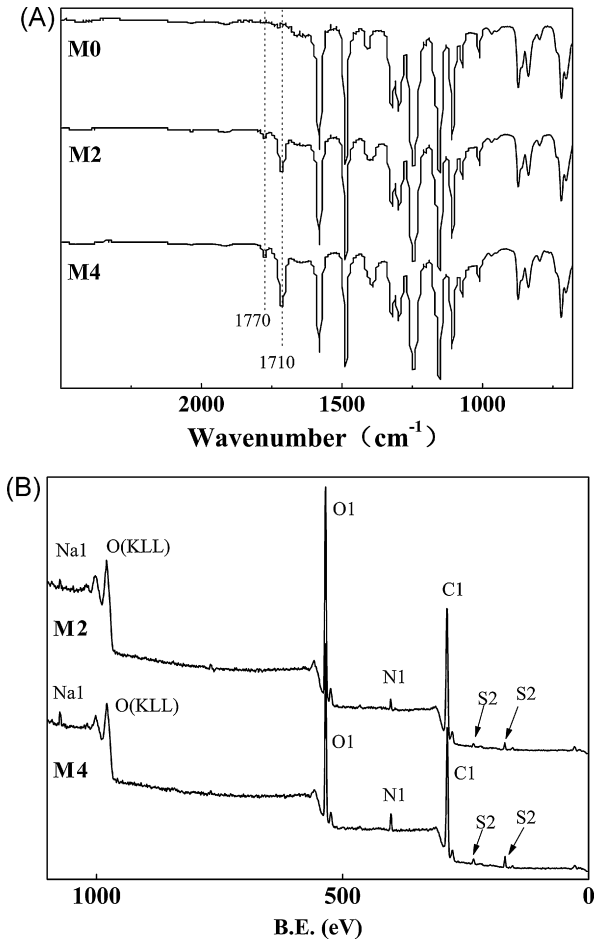

Fig. 3. (A) ATR-FTIR spectra of the membrane surfaces (M0, M2 and M4) and (B) XPS spectra of the membrane surfaces (M2 and M4).

Moreover, the solubility test showed that the derivatives of chitosan (OC and SOC) were soluble in common solvents such as DMF, DMAc and DMSO, which were also confirmed by the results of X-ray diffraction.

3.2. Characterization of the membranes

3.2.1. ATR-FTIR and XPS analysis

ATR-FTIR spectra for the surfaces of PES and PES/SOC membranes are shown in Fig. 3A. The most significant changes for the modified membranes were the appearance of the characteristic peaks at about 1710 and 1770 cm^{-1}, which were the characteristic peaks of the derivative of chitosan (SOC). Fig. 3B presents the XPS spectrum of the PES/SOC membranes surface at an X-ray take-off angle of 20°. As shown in Fig. 3B and supplementary Table S2, the element contents of N and S for the modified membrane surfaces were increased significantly compared to pure PES membrane (Zhao et al., 2012). Furthermore, the element contents of N and S for the membrane were increased with the increase of the content of SOC. Thus, a conclusion could be drawn that SOC with different contents had been blended into PES membranes successfully.

3.2.2. Water contact angle analysis

The surface hydrophilicity was determined by dynamic contact angle measurements, and the data are illustrated in Fig. 4. It could be found that the stationary, advancing, and receding contact angles for the modified membranes are smaller than that for the pristine PES membrane and the values decreased with the increase

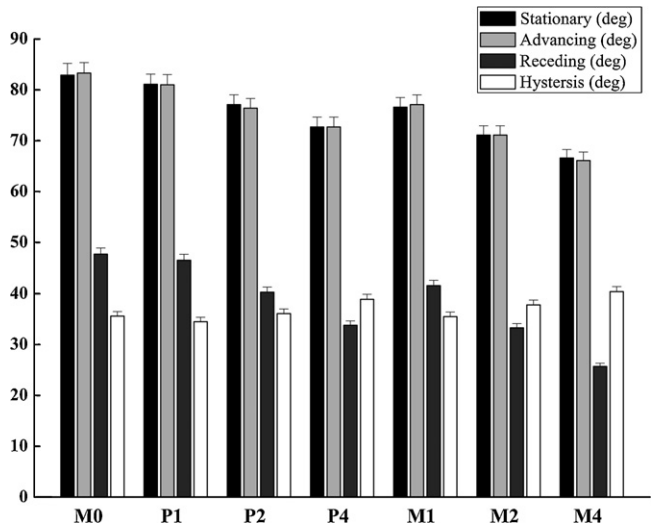

Fig. 4. Dynamic contact angles for the membranes.

of the OC/SOC amounts in the membranes, especially for PES/SOC membrane. It was indicated that the surface hydrophilicity of the blended membranes increased with the incorporation of OC/SOC. Membrane M4 had the highest hysteresis, which was attributed to the lower degree of phase mixing and higher degree of surface rearrangement upon water contact (Grapski & Cooper, 2001; Yung & Cooper, 1998).

3.2.3. Morphology of the modified membranes (SEM)

The cross-sectional SEM micrographs of pristine and blended PES membranes are shown in supplementary Fig. S1. The characteristic morphology of PES membrane was observed, consisting of a thin dense skin layer at the top side, a finger-like structure and porous architecture at the bottom (Qian et al., 2009). For the modified membranes, the pore diameter of finger-like structure increased and expanded to the bottom, and the number of macrovoid decreased with the increase of the content of SOC/OC. Boom, Wienk, Van den Boomgaard, and Smolders (1992) had explained that the addition of a high molecular weight polymer to a casting dope would suppress the macrovoid formation. Moreover, large numbers of micropores on the surface of the macrovoids were observed in M4 sample, which was caused by the hydrophilic groups of the derivative of chitosan in the casting dope (Huang et al., 2011).

3.3. Blood compatibility of the membrane

It must be noted that, although the common methods: protein adsorption, platelet adhesion and clotting time were tested here, it is as yet not possible to make a conclusion with respect to the overall improvement of membranes blood compatibility, since the limitations of conditions to use standardized methods to assess blood compatibility of materials or to focus on the whole blood system rather than considering the individual aspects of that (Gorbet & Sefton, 2004; Ratner, 2007).

3.3.1. Protein adsorption

It is well known that protein adsorption was one of the important factors to evaluate the blood compatibility of materials. Since protein adsorption is the first event in blood–material interactions and some proteins in blood, especially the clotting enzymes and fibrinogen (Brash & Horbett, 1995). Moreover, fibrinogen in blood plasma is particularly important for platelet adhesion since

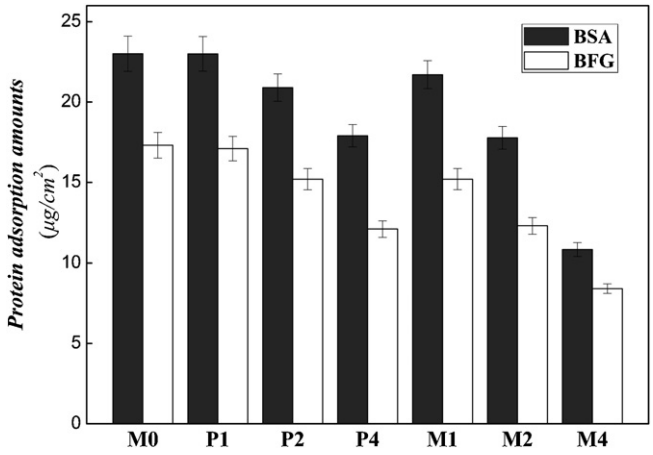

Fig. 5. BSA and BFG adsorbed amounts on the membranes. Values are expressed as means ± SD, $n = 3$.

it can bind to the platelet GP IIb/IIIa receptor (Tsai, Grunkemeier, McFarland, & Horbett, 2002).

As shown in Fig. 5, it was found that all the blended PES membranes had lower BSA and BFG adsorption than the pristine membrane, and the PES/SOC membranes had lower adsorption compared to PES/OC membranes as the same incorporation of additive. Furthermore, the values decreased with the increase of OC or SOC contents in the membranes. It indicated that the increased hydrophilicity of the modified membrane surface and the electrostatic repulsion of the negatively charged surface are the key factors to surface resistence to protein adsorption. Zhang et al. (2008) explained that the molecular units of the hydrophilic surface have the ability to tightly bind structure water, and then the tightly bound surface water may be responsible for the low protein adsorption at low protein solution concentrations.

3.3.2. Platelet adhesion

Platelet adhesion is mediated by integrins on the surface of the platelet and cause platelet activation, and then the activated platelets accelerate thrombosis as they promote thrombin formation and platelet aggregation (Grunkemeier, Tsai, McFarland, & Horbett, 2000; Nygren & Broberg, 1998). Thus, the platelet adhesion test was important to investigate the blood compatibility for biomedical materials.

The scanning electron micrographs of the adhering platelets on the membranes are shown in Fig. 6. It could be found that numerous platelets were accumulated on the surface of PES membrane, and spread in flattened and irregular shapes; moreover, pseudopodia were observed. Whereas the number of platelets adhered on the blended membranes was reduced substantially than that on the pristine PES membrane, especially for PES/SOC membranes and almost no adhered platelet was observed on the surface of M4, as shown in Fig. 6b. Moreover, the shapes of platelets adhered on PES/SOC were better than that of PES/OC. This should be attributed to the relatively low protein adsorption and the improved hydrophilicity of the modified membranes. It was reported that the adsorbed proteins, especially fibrinogen, played a critical role in platelet adhesion, though it was not clear, for example, how effective the adsorbed fibrinogen was as a platelet agonist in vivo and what other mechanisms were involved in supporting or initiating platelet adhesion (Gorbet & Sefton, 2004). Thus, the low protein adsorption and suppressed platelet adhesion indicated that the blood compatibility of the membranes was improved to some extent.

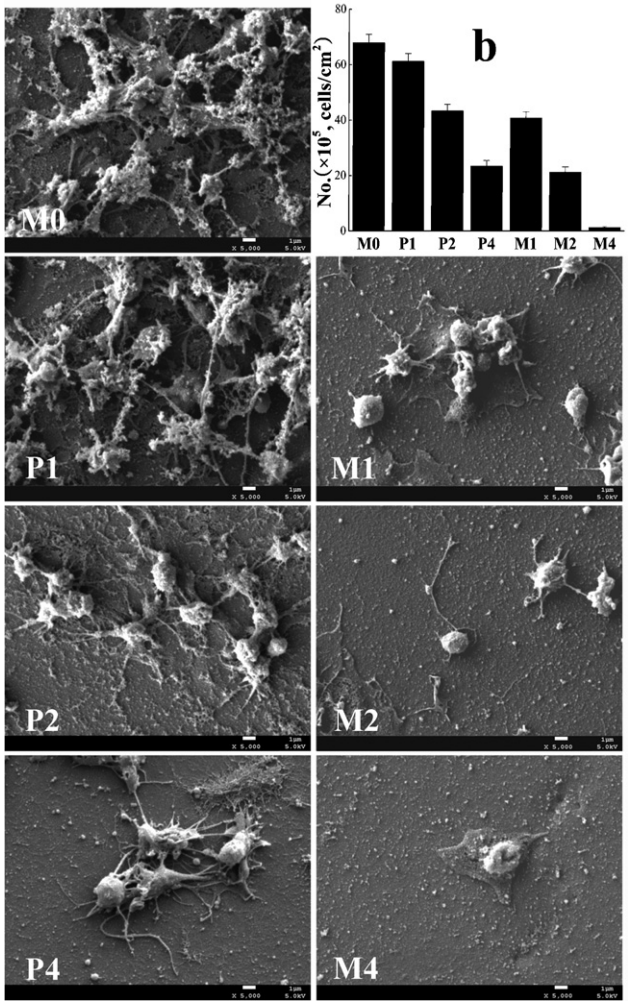

Fig. 6. Typical scanning electron micrographs of the platelets adhering on the membranes; magnification: 5000×. (b) Number of the adherent platelets on the membranes estimated from the SEM pictures.

3.3.3. Clotting time (APTT and TT)

The activated partial thromboplastin time (APTT) and thrombin time (TT) tests were widely used for the clinical detection of the abnormality of blood plasma and for the primary screening of the anticoagulative chemicals; recently, these tests were applied in the evaluation of the in vitro antithrombogenicity of biomaterials (Huang, Du, Yang, & Fan, 2003; Li et al., 2009; Lin, Liu, & Yang, 2004), since the length of APTT reflected the levels of prothrombin, fibrinogen and blood coagulation factors V and X in plasma in endogenous pathway of coagulation. When an anticoagulative material contacted with blood, it might combine or react with the coagulation factors, and the APTT could be prolonged. TT was mainly affected by the content of fibrinogen and fibrin in plasma and coagulation activity. The TT reflected the level of common pathway of coagulation (Fu et al., 2011).

The clotting times for the derivatives of chitosan and the membranes are shown in Fig. 7, and all the results were analyzed by statistical methods (significant difference, $P < 0.05$). For SOC (Fig. 7A), the APTT increased sharply with the increment of the concentration of the derivative of chitosan than OC. This might be attributed to the reaction or combination between the coagulation factors (V and X) in plasma and the sulfated derivative of chitosan, the high level of negative charge density produced by the sulfate groups and the decreased positive charge density of amino groups. Compared to the APTT, the TT increased slightly, which was

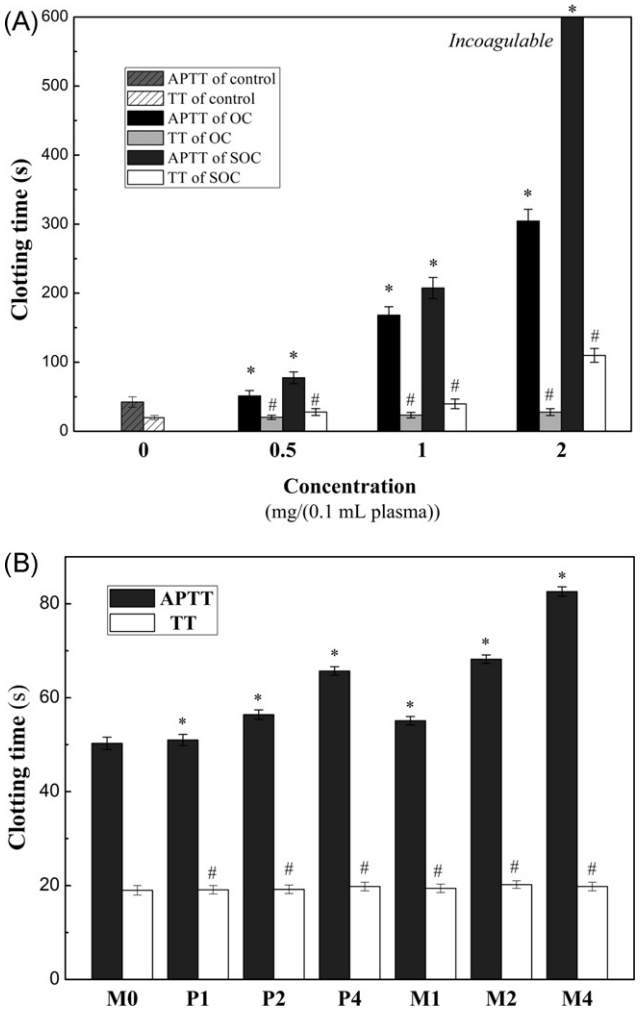

Fig. 7. (A) APTT and TT for the derivatives of chitosan ($^{*}P<0.05$ and $^{\#}P<0.05$ compared with plasma); (B) APTT and TT for the membranes ($^{*}P<0.05$ and $^{\#}P<0.05$ compared with pristine PES membrane).

in agreement with the previous study (Huang et al., 2003), the slight increase of TT might be attributed to the low S wt.%. Moreover, the regular arrangement of the sulfate groups was more beneficial to TT anticoagulant activity of the sulfated polysaccharides in comparison to that of APTT. The slight increase of APTT and TT for OC was attribute to the less content of the carboxyl groups.

For the blended membranes, as shown in Fig. 7B, the APTTs increased compared with that for the pristine PES membrane; moreover, with the increase of the derivatives of chitosan amounts in the membranes, the APTT increased. The APTT for M4 was enhanced as high as 60% compared to pure PES membrane. For most synthetic materials, the presence of adherent platelets usually decrease the plasma clotting time due to the platelet catlayze thrombin formation, i.e. they are procoagulant (Zhang et al., 2008). Morevoer, the prolonged APTT also might be attributed to the increased hydrophilicity, lower protein adsorption. However, the TT of the modified membrane showed slightly changes, this was consistent with the results of the derivatives of chitosan mentioned above.

3.4. Permeation and antifouling property

The protein antifouling property of the membranes was studied by ultrafiltration experiments. Supplementary Fig. S2 shows the time-dependent flux during the ultrafiltration. As shown in the figure, the water fluxes ranged from 28.5 to 247.6 mL/(m^2 h mmHg) for the membranes. This was caused by the different membrane hydrophilicity after blending the derivatives of chitosan.

A considerable reduction of flux was observed when the solution changed from water to BSA solution due to the membrane fouling caused by the deposition and adsorption of protein molecules onto the membrane surfaces and/or in the membrane pores. When the adsorption and deposition of protein molecules became saturated, a relatively steady flux was obtained. The fluxes of the blended membranes were higher compared to that of the pristine membrane. It was caused by the increased hydrophilicity and larger pore diameter, which could be observed from the SEM pictures (supplementary Fig. S1). The BSA rejection ratios were calculated and the values were similar for all the membranes (supplementary Table S3), which indicated that there was no significant difference in the dense layers of membranes.

When the solution changed from BSA solution to water, the fluxes of the membranes were recovered to some extent. The water flux recovery ratio (F_{RR}) is also shown in supplementary Table S3. It was observed that the blended membranes had higher F_{RR} value than that of pristine membrane and the value was increased with the increase of the derivatives amounts, since the improved hydrophilicity and charge interactions of blended membranes decreased the protein adsorption, leading to the decrease in protein fouling. Furthermore, a long-term ultrafiltration with three runs was carried out to investigate the recycling property of the modified membranes. After three cycles of BSA ultrafiltration, the flux recovery ratio was about 80.1% for M4. These results indicated the modified membranes have a good anti-fouling property.

4. Conclusions

A new sulfated derivative of chitosan, which could be dissolved in common organic solvents, was synthesized for the first time by a simple and convenient method. The sulfated derivate of chitosan can be directly blended with PES to prepare modified PES membranes. The modified membranes have better blood compatibility (BSA and BFG adsorption, platelet adhesion, and blood coagulation time) compared with the pristine PES membrane after blending with the sulfated derivative of chitosan. Moreover, the modified membranes showed good ultrafiltration and protein anti-fouling properties. These results indicated that the modified membranes have the potential to be used in blood puification including hemodialysis and bioartificial liver supports.

Acknowledgements

This work was financially sponsored by the National Natural Science Foundation of China (Nos. 51073105, 51173119 and 51225308), State Education Ministry of China (Doctoral Program for High Education, No. 20100181110031), and Program for Changjiang Scholars and Innovative Research Team in University (IRT1163). We should also thank our laboratory members for their generous help, and gratefully acknowledge the help of Ms. H. Wang, of the Analytical and Testing Center at Sichuan University, for the SEM, and Ms. Liang, of the Department of Nephrology at West China Hospital, for the human fresh blood collection.

Appendix A. Supplementary data

Supplementary data associated with this article can be found, in the online version, at http://dx.doi.org/10.1016/j.carbpol.2013.02.033.

References

Boom, R. M., Wienk, I. M., Van den Boomgaard, T., & Smolders, C. A. (1992). Microstructures in phase inversion membranes. Part 2. The role of a polymeric additive. *Journal of Membrane Science*, *73*, 277–292.

Brash, J. L., & Horbett, T. A. (1995). *Proteins at interfaces II* Washington, DC: ACS Publications., pp. 1–23, (Chapter 1)

Chaudhari, L. B., & Murthy, Z. (2011). Post-treatment of biologically treated wastewater of agrochemical industry by sulfated chitosan composite nanofiltration membrane. *Water Science & Technology*, *64*, 796–802.

Fang, B. H., Ling, Q. Y., Zhao, W. F., Ma, Y. L., Bai, P. L., Zhao, C. S., et al. (2009). Modification of polyethersulfone membrane by grafting bovine serum albumin on the surface of polyethersulfone/poly (acrylonitrile-co-acrylic acid) blended membrane. *Journal of Membrane Science*, *329*, 46–55.

Fu, D. W., Han, B. Q., Dong, W., Yang, Z., Lv, Y., & Liu, W. S. (2011). Effects of carboxymethyl chitosan on the blood system of rats. *Biochemical and Biophysical Research Communications*, *408*, 110–114.

Gorbet, M. B., & Sefton, M. V. (2004). Biomaterial-associated thrombosis: Roles of coagulation factors, complement, platelets and leukocytes. *Biomaterials*, *25*, 5681–5703.

Grapski, J. A., & Cooper, S. L. (2001). Synthesis and characterization of non-leaching biocidal polyurethanes. *Biomaterials*, *22*, 2239–2246.

Grunkemeier, J. M., Tsai, W. B., McFarland, C. D., & Horbett, T. A. (2000). The effect of adsorbed fibrinogen, fibronectin, von Willebrand factor and vitronectin on the procoagulant state of adherent platelets. *Biomaterials*, *21*, 2243–2252.

Huang, R. H., Du, Y. M., Yang, J. H., & Fan, L. H. (2003). Influence of functional groups on the in vitro anticoagulant activity of chitosan sulfate. *Carbohydrate Research*, *338*, 483–489.

Huang, R. H., Du, Y. M., Zheng, L. S., Liu, H., & Fan, L. H. (2004). A new approach to chemically modified chitosan sulfates and study of their influences on the inhibition of *Escherichia coli* and *Staphylococcus aureus* growth. *Reactive and Functional Polymers*, *59*, 41–51.

Huang, J. Y., Xue, J. M., Xiang, K. W., Zhang, X., Sun, S. D., Zhao, C. S., et al. (2011). Surface modification of polyethersulfone membranes by blending triblock copolymers of methoxyl poly (ethylene glycol)-polyurethane-methoxyl poly (ethylene glycol). *Colloids and Surfaces B: Biointerfaces*, *88*, 315–324.

Karadeniz, F., Karagozlu, M. Z., Pyun, S. Y., & Kim, S. K. (2011). Sulfation of chitosan oligomers enhances their anti-adipogenic effect in 3T3-L1 adipocytes. *Carbohydrate Polymers*, *86*, 666–671.

Kurita, K., Ikeda, H., Yoshida, Y., Shimojoh, M., & Harata, M. (2002). Chemoselective protection of the amino groups of chitosan by controlled phthaloylation: Facile preparation of a precursor useful for chemical modifications. *Biomacromolecules*, *3*, 1–4.

Li, J., Zhu, B. Q., Shao, Y. Y., Liu, X. R., Yang, X. L., & Yu, Q. (2009). Construction of anticoagulant poly (lactic acid) films via surface covalent graft of heparin-carrying microcapsules. *Colloids and Surfaces B: Biointerfaces*, *70*, 15–19.

Lin, W. C., Liu, T. Y., & Yang, M. C. (2004). Hemocompatibility of polyacrylonitrile dialysis membrane immobilized with chitosan and heparin conjugate. *Biomaterials*, *25*, 1947–1957.

Matsuyama, H., Nishiguchi, M., & Kitamura, Y. (2000). Phase separation mechanism during membrane formation by dry-cast process. *Journal of Applied Polymer Science*, *77*, 776–783.

Muzzarelli, R. A. A., & Giacomelli, G. (1987). The blood anticoagulant activity of *N*-carboxymethylchitosan trisulfate. *Carbohydrate Polymers*, *7*, 87–96.

Muzzarelli, R. A. A., Tanfani, F., Emanuelli, M., P Pace, D., Chiurazzi, E., & Piani, M. (1984). Sulfated *N*-(carboxymethyl) chitosans: Novel blood anticoagulants. *Carbohydrate Research*, *126*, 225–231.

Nishimura, S., Kohgo, O., Kurita, K., & Kuzuhara, H. (1991). Chemospecific manipulations of a rigid polysaccharide: Syntheses of novel chitosan derivatives with excellent solubility in common organic solvents by regioselective chemical modifications. *Macromolecules*, *24*, 4745–4748.

Nygren, H., & Broberg, M. (1998). Specific activation of platelets by surface-adsorbed plasma proteins. *Journal of Biomaterials Science, Polymer Edition*, *9*, 817–831.

Qian, B. S., Li, J., Wei, Q., Bai, P. L., Fang, B. H., & Zhao, C. S. (2009). Preparation and characterization of pH-sensitive polyethersulfone hollow fiber membrane for flux control. *Journal of Membrane Science*, *344*, 297–303.

Ran, F., Nie, S. Q., Zhao, W. F., Li, J., Sun, S. D., Zhao, C. S., et al. (2011). Biocompatibility of modified polyethersulfone membranes by blending an amphiphilic triblock co-polymer of poly(vinyl pyrrolidone)-b-poly(methyl methacrylate)-b-poly(vinyl pyrrolidone). *Acta Biomater*, *7*, 3370–3381.

Ratner, B. D. (2007). The catastrophe revisited: Blood compatibility in the 21st century. *Biomaterials*, *28*, 5144–5147.

Saito, H., Tabeta, R., & Ogawa, K. (1987). High-resolution solid-state carbon-13 NMR study of chitosan and its salts with acids: Conformational characterization of polymorphs and helical structures as viewed from the conformation-dependent carbon-13 chemical shifts. *Macromolecules*, *20*, 2424–2430.

Samtleben, W., Dengler, C., Reinhardt, B., Nothdurft, A., & Lemke, H. D. (2003). Comparison of the new polyethersulfone high-flux membrane DIAPES® HF800 with conventional high-flux membranes during on-line haemodiafiltration. *Nephrology Dialysis Transplantation*, *18*, 2382–2386.

Sperling, C., Houska, M., Brynda, E., Streller, U., & Werner, C. (2006). In vitro hemocompatibility of albumin-heparin multilayer coatings on polyethersulfone prepared by the layer-by-layer technique. *Journal of Biomedical Materials Research Part A*, *76A*, 681–689.

Tsai, W. B., Grunkemeier, J. M., McFarland, C. D., & Horbett, T. A. (2002). Platelet adhesion to polystyrene-based surfaces preadsorbed with plasmas selectively depleted in fibrinogen, fibronectin, vitronectin, or von Willebrand's factor. *Journal of Biomedical Materials Research*, *60*, 348–359.

Vikhoreva, G., Bannikova, G., Stolbushkina, P., Panov, A., Drozd, N., Gal'braikh, L., et al. (2005). Preparation and anticoagulant activity of a low-molecular-weight sulfated chitosan. *Carbohydrate Polymers*, *62*, 327–332.

Vongchan, P., Sajomsang, W., Subyen, D., & Kongtawelert, P. (2002). Anticoagulant activity of a sulfated chitosan. *Carbohydrate Research*, *337*, 1239–1242.

Yang, J. H., Cai, J., Wu, K., Li, D. L., Hu, Y., Du, Y. M., et al. (2012). Preparation, characterization and anticoagulant activity in vitro of heparin-like 6-carboxylchitin derivative. *International Journal of Biological Macromolecules*, *50*, 1158–1164.

Yung, L. Y. L., & Cooper, S. L. (1998). Neutrophil adhesion on phosphorylcholine-containing polyurethanes. *Biomaterials*, *19*, 31–40.

Zhang, Z., Zhang, M., Chen, S. F., Horbett, T. A., Ratner, B. D., & Jiang, S. Y. (2008). Blood compatibility of surfaces with superlow protein adsorption. *Biomaterials*, *29*, 4285–4291.

Zhao, C. S., & Li, T. (2001). An evaluation of a polyethersulfone hollow fiber plasma separator by animal experiment. *Artificial Organs*, *25*, 60–63.

Zhao, W. F., Mou, Q. B., Zhang, X. X., Shi, J. Y., Sun, S. D., & Zhao, C. (2012). Preparation and characterization of sulfonated polyethersulfone membranes by a facile approach. *European Polymer Journal*, http://dx.doi.org/10.1016/j.eurpolymj.2012.11.018